

# Neuronal origin of a cerebral amyloid: neurofibrillary tangles of Alzheimer's disease contain the same protein as the amyloid of plaque cores and blood vessels

Colin L.Masters<sup>1,2</sup>, Gerd Multhaup<sup>3</sup>, Gail Simms<sup>1</sup>, Jutta Pottgiesser<sup>3</sup>, Ralph N.Martins<sup>1</sup> and Konrad Beyreuther<sup>3</sup>

<sup>1</sup>Laboratory of Molecular and Applied Neuropathology, Neuromuscular Research Institute, Department of Pathology, University of Western Australia, Western Australia 6009, and <sup>2</sup>Department of Neuropathology, Royal Perth Hospital, Perth, Western Australia 6001, and <sup>3</sup>Institute for Genetics, University of Cologne, Weyertal 121, D-5000 Cologne 41, FRG

Communicated by K.Beyreuther

**The protein component of Alzheimer's disease amyloid [neurofibrillary tangles (NFT), amyloid plaque core and congophilic angiopathy] is an aggregated polypeptide with a subunit mass of 4 kd (the A<sub>4</sub> monomer). Based on the degree of N-terminal heterogeneity, the amyloid is first deposited in the neuron, and later in the extracellular space. Using antisera raised against synthetic peptides, we show that the N terminus of A<sub>4</sub> (residues 1–11) contains an epitope for neurofibrillary tangles, and the inner region of the molecule (residues 11–23) contains an epitope for plaque cores and vascular amyloid. The non-protein component of the amyloid (aluminum silicate) may form the basis for the deposition or amplification (possible self-replication) of the aggregated amyloid protein. The amyloid of Alzheimer's disease is similar in subunit size, composition but not sequence to the scrapie-associated fibril and its constituent polypeptides. The sequence and composition of NFT are not homologous to those of any of the known components of normal neurofilaments.**

**Key words:** protein sequence/h.p.l.c./scrapie/aluminum silicate/Alzheimer's disease

## Introduction

Alzheimer's disease (AD) is the commonest form of cerebral degeneration leading to dementia in late adult life. The peak incidence occurs in the eighth decade, and the average duration of illness is 6 years, steadily progressing without remission or relapse. The pathognomonic changes in the AD brain are the formation of fibrillar amyloid deposits in intracellular and extracellular locations: intracellular neurofibrillary tangles (NFT) composed of paired helical filaments (PHF) within neurons and within pre-synaptic axonal terminals surrounding extracellular deposits of amyloid plaque cores (APC), and a variable degree of amyloid congophilic angiopathy (ACA). There is also widespread neuronal loss and gliosis in areas affected by NFT and APC formation. These typical changes of AD also occur in the brains of aged individuals with Down's syndrome (DS).

Although the cause of AD is unknown, it shares many features with the unconventional virus diseases [Creutzfeldt-Jakob disease (CJD), kuru and scrapie] (Masters *et al.*, 1981a, 1981b), but not least of which are the occurrence of amyloid plaques (Masters *et al.*, 1981b); the similarities in morphology between amyloid fibrils, PHF and scrapie-associated fibrils (SAF) (Merz *et al.*, 1981; DeArmond *et al.*, 1985), the Congo Red binding properties of SAF (Prusiner *et al.*, 1983); the immunological cross-reactivity between scrapie-associated proteins and scrapie amyloid

plaques (Bendheim *et al.*, 1984; DeArmond *et al.*, 1985); the observation that a method used to purify SAF when applied to an AD brain will yield PHF (Rubenstein *et al.*, 1985); and that the size and amino acid composition of the scrapie-associated proteins are consistent with amyloid proteins in general (Multhaup *et al.*, 1985).

As a first step in understanding the pathogenesis of AD, we recently isolated and characterized the protein component of the APC (Masters *et al.*, 1985), and found it to consist of aggregates of a 4-kd polypeptide (A<sub>4</sub> monomer, A<sub>8</sub> dimer, A<sub>16</sub> tetramer, A<sub>64</sub> hexadecamer), similar in amino acid composition and sequence to ACA (Glennner and Wong, 1984). However the APC-A<sub>4</sub> was found to have ragged N termini, in contrast to ACA-A<sub>4</sub> which was reported as being composed of only the full length major sequence. The same A<sub>4</sub> protein was found to be the constituent of the APC and ACA of DS (Masters *et al.*, 1985; Glennner and Wong, 1984).

We have now examined the composition of purified NFT-AD, and report that they contain the same A<sub>8</sub>, A<sub>16</sub> and A<sub>64</sub> oligomeric species of the A<sub>4</sub> monomer as found in APC and ACA. The N termini of the NFT protein are even more ragged than found for APC. From these observations we can draw several conclusions on the probable pathogenesis of NFT, APC and ACA. Since the subunit protein of SAF is now also known in some detail (Multhaup *et al.*, 1985; Oesch *et al.*, 1985), comparisons can be drawn between the various forms of cerebral amyloid proteins.

## Results and Discussion

### Isolation of NFT

The enriched fractions of NFT (Figure 1) contain lipofuscin and collagen as the major contaminants. Some APC and fragments thereof are seen by electron microscopy, but overall 50–90% of the fraction consists of NFT, as judged by light and electron microscopy. The purity of the preparations varies from case to case, and from those individuals with the greatest numbers of NFT (enumerated by histology of the contralateral hemisphere) the highest and cleanest yields of NFT are obtained.

### NFT and APC are composed of the A<sub>4</sub> protein subunit

The protein component of NFT was extracted with 100% formic acid. To assess the degree of protein solubilization, we used quantitative amino acid analysis of HCl-hydrolysates of NFT before and after formic acid extraction. More than 90% of the NFT protein was soluble in formic acid, and the amino acid compositions of total NFT protein before and after extraction were almost indistinguishable (Table I). SDS (0.1–10%) does not solubilize the NFT proteins in their native state, a property shared with the APC proteins (Masters *et al.*, 1985). However, once extracted in formic acid and thus separated from non-proteinaceous components, these proteins are soluble in 0.1% SDS buffers, but are still not dissociated into monomeric subunits, until treated with 6 M urea. When electrophoresed in SDS-urea polyacrylamide gels, the 4-kd monomer is seen, identical to the APC-A<sub>4</sub> protein (Figure 2).

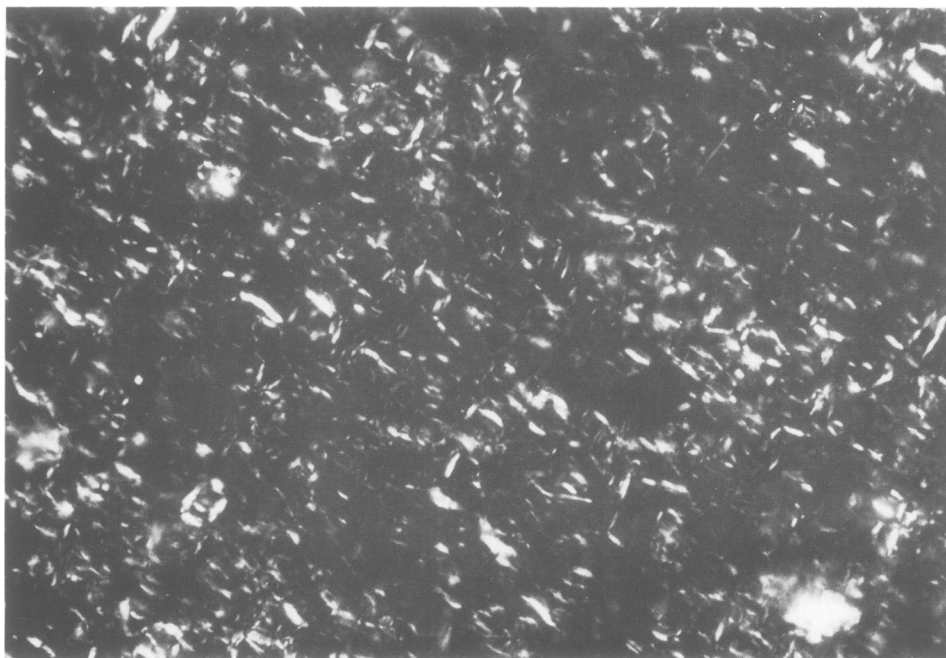


**Fig. 1.** An enriched fraction NFT stained with Congo Red and viewed with polarization light microscopy. Most of the negatively birefringent material is elongated and flame-shaped, typical of intracellular accumulations of NFT. (Magnification X 550).

**Table I.** Amino acid composition of NFT and APC proteins

Amino acid	nmol residues <sup>a</sup>		mol %		H.p.l.c. fractions of formic acid extracts			Number of residues per monomer		
	Total NFT	Formic acid extract of NFT	Total NFT	Formic acid extract of NFT				NFT A <sub>8</sub>	APC <sup>c</sup> A <sub>4</sub>	Scrapie-associated protein <sup>d</sup> (7 kd)
					A <sub>64</sub>	A <sub>16</sub>	A <sub>8</sub>			
Asp	2.08	2.07	7.74	8.12	8.51	8.46	8.52	3.41	4	6
Thr	1.28	0.88	4.76	3.45	3.35	1.62	2.73	1.09	(1)	4
Ser	2.07	1.65	7.70	6.47	7.86	6.23	7.83	3.13	3	3
Glu	2.93	2.62	10.90	10.28	11.46	11.97	12.47	5.00	5	6
Pro	0.77	0.77	2.87	3.02	1.66	1.87	3.38	1.35	(1)	3
Cys	0.95	0.93	3.53	3.64	+	+	+	(1)	(1)	(1)
Gly	3.24	3.09	12.05	12.12	15.63	15.09	15.60	6.64	6	7
Ala	1.82	1.63	6.77	6.39	8.21	8.98	8.27	3.31	4	4
Val	1.52	1.69	5.65	6.63	9.28	10.47	8.36	3.34	4	3
Met	0.39	0.47	1.45	1.84	1.69	1.51	1.21	0.48	1	3
Ile	1.23	1.00	4.58	3.92	4.85	4.99	4.03	1.61	2	2
Leu	2.09	2.00	7.78	7.84	7.09	6.86	6.75	2.70	3	4
Tyr	0.73	0.82	2.72	3.22	2.19	2.49	2.21	0.88	1	3
Phe	1.60	1.86	5.95	7.29	4.57	6.36	3.90	1.56	3	2
His	0.71	0.96	2.64	3.76	3.74	4.86	4.03	1.61	3	2
Lys	2.22	1.77	8.26	6.94	7.09	5.74	7.27	2.91	2	3
Arg	1.20	1.29	4.46	5.06	2.82	2.50	3.38	1.35	1	3
GlcN	0.05	0.05	0.11	0.20	0	0	0	0	0	(8)
nmol protein	0.60 (100%)	0.57 (95%)	0.60	0.57	0.51	0.25	0.23			
Total								41	45	59

<sup>a</sup>For 2.5 µg of NFT protein.

<sup>b</sup>Tryptophan was not determined.

<sup>c</sup>Calculated composition of the A<sub>4</sub> subunit of APC from AD and DS individuals (Masters *et al.*, 1985).

<sup>d</sup>Deduced for the CLAC strain of the 7-kd deglycosylated hamster scrapie-associated protein (Multhaup *et al.*, 1985).

#### *NFT- and APC-A<sub>4</sub> subunits aggregate into dimers, tetramers and hexadecamers*

After solubilization in formic acid, the NFT protein can be chromatographed in 0.1 % SDS buffers. By h.p.l.c. gel permea-

tion chromatography, the NFT proteins have mol. wts. of 64, 16 and 8 kd (A<sub>64</sub>, A<sub>16</sub>, A<sub>8</sub>) (Figure 3a). The NFT-A<sub>64</sub> is dissociated into NFT-A<sub>8</sub> after formic acid treatment prior to re-chromatography (Figure 3c). NFT-A<sub>16</sub> can also be broken down to A<sub>8</sub> species after re-extraction with formic acid (data not

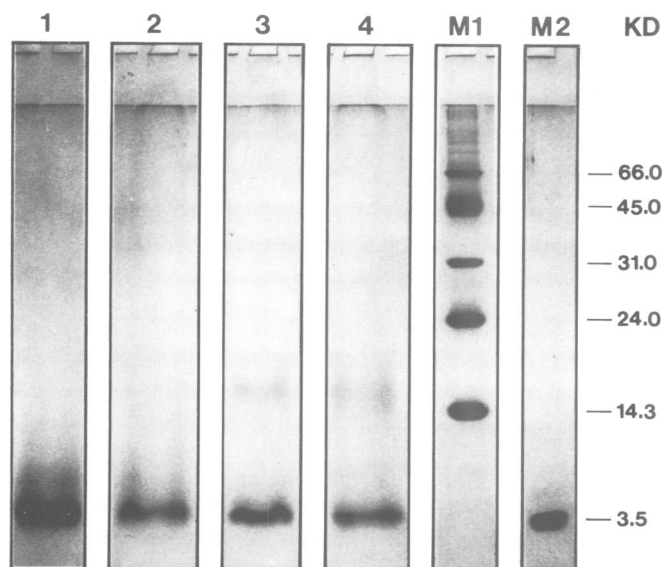


**Fig. 2.** Gel electrophoresis of NFT and APC proteins. SDS/urea polyacrylamide gel electrophoresis of formic acid extracts of oxidized NFT proteins (12.2  $\mu$ g, lane 1), oxidized APC proteins (9.6  $\mu$ g, lane 2), NFT proteins (12.2  $\mu$ g, lane 3) and APC proteins (9.6  $\mu$ g, lane 4). Lanes M1 and M2 are marker proteins. Both NFT and APC proteins behave in the same electrophoretic manner — most of the protein migrates as the  $A_4$  monomer.

shown). Thus, NFT- $A_{64}$ ,  $A_{16}$  and  $A_8$  appear to be hexadecamers, tetramers and dimers of 4-kd subunits. The APC proteins have identical aggregational properties (Masters *et al.*, 1985 and Figure 3).  $A_8$  dimers of both NFT and APC are not dissociated into monomers by either SDS or formic acid. But urea and SDS together will lead to dissociation into  $A_4$  monomers (Figure 2).  $A_8$  dimers are seen as faint bands in SDS-urea gels of freshly prepared material (Figure 2) and as more prominent bands from preparations that have been left at room temperature for some time (Masters *et al.*, 1985).

Are the amyloid fibril proteins stabilized by interchain S-S bridges? The amino acid compositions of NFT- and APC- $A_4$  indicate the presence of one half cystine per chain (Table I). Performic acid treatment of NFT and APC proteins prior to gel electrophoresis does not cause any appreciable change, suggesting that the native tangle and plaque core  $A_4$  proteins are devoid of interchain disulfide linkages (Figure 2). Both APC- and NFT- $A_4$  monomers show the same pH- and concentration-dependent aggregation. At pH values  $>7$ , higher aggregates dominate and little  $A_{16}$  and  $A_8$  species are detected by h.p.l.c. in buffers containing SDS. This aggregation tendency is completely changed at pH values  $<7$ , and almost no  $A_{64}$  species are seen if the protein concentration is kept below 0.1 mg/ml. Above this concentration, the excess protein almost exclusively occurs as an increase in the  $A_{64}$  peak, whereas the  $A_8$  and  $A_{16}$  peaks remain relatively constant.

#### *The amino acid composition and sequences of NFT and APC proteins are the same*

The amino acid composition of NFT- $A_4$  (as deduced from the compositions of NFT- $A_{64}$ ,  $A_{16}$ ,  $A_8$  and whole NFT) is very similar to APC- $A_4$  (Table I). This alone suggested that the NFT- $A_4$  and APC- $A_4$  were the same protein. Gas-liquid solid phase sequencing of unfractionated NFT protein and NFT- $A_8$  confirms the identity of the NFT and APC proteins (Figure 4). The N-terminal sequence of the NFT proteins shows a large degree of heterogeneity (Figure 4); more heterogeneous, in fact, than seen for the APC protein. If, as reported by Glenner and Wong (1984),

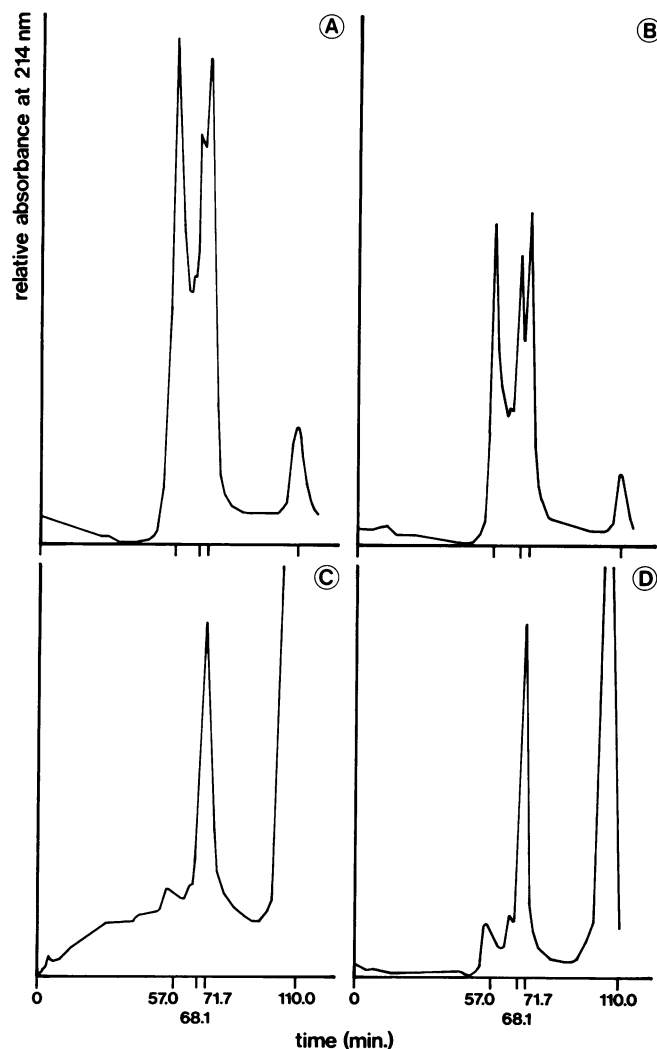


**Fig. 3.** H.p.l.c. gel permeation chromatography of NFT and APC proteins. Proteins [25  $\mu$ g of NFT protein (A) and 12.5  $\mu$ g of APC protein (B)] obtained by formic acid extraction of purified whole NFT or APC were lyophilized, re-dissolved in 50  $\mu$ l of h.p.l.c. buffer and chromatographed at a flow-rate of 0.2 ml/min. The peaks eluting at 57.0 min, 68.1 min and 71.7 min correspond to proteins of mol. wt. 64 kd ( $A_{64}$ ), 16 kd ( $A_{16}$ ) and 8 kd ( $A_8$ ), as deduced from the elution times of marker proteins. The peak at 110 min is the salt front. Protein peaks were collected, lyophilized, re-dissolved in formic acid, lyophilized again and taken up in 50  $\mu$ l of h.p.l.c. buffer for re-chromatography. (C) is the re-chromatographic profile of the NFT- $A_{64}$  peak from (A). (D) is the re-chromatographic profile of the APC- $A_{64}$  peak from (B).

the ACA protein exhibits complete N-terminal homogeneity (Figure 4), then we may postulate that the NFT protein is chronologically the oldest, the APC protein is intermediate, and that the ACA protein is the most recently deposited form of the three types of cerebral amyloid. One ought not to forget that the amyloid proteins of AD may have age ranges extending over two orders of magnitude from 50 to 5000 days, at least based on the known durations of the clinical disease. The N-terminal heterogeneity also excludes the possibility that residues 1–11 of the  $A_4$  molecule are involved in the aggregational properties of the monomer.

#### *NFT, APC and ACA share differential antigenic determinants within the $A_4$ monomer*

Most rabbits immunized with whole APC eventually respond by producing antibodies which react with both APC and ACA

(Figure 5a, b). Two rabbits immunized with APC [one with alkali-degraded material, the other with sonicated APC coupled to keyhole limpet haemocyanin (KLH)] responded by making antibodies to NFT and not APC or ACA, as did one rabbit immunized with the h.p.l.c.-derived  $A_{16}/A_8$  peaks from an APC preparation (Figure 5c). The NFT stained in the sections of AD brain are restricted to the cell soma, and appear to be a select population, as some NFT within the hippocampal regions were not reactive. Antisera raised against the synthetic peptide corresponding to the intact N terminus of the  $A_4$  monomer [SP  $A_4(1-11)$ ] also stained NFT in AD brain sections. However, antisera raised against the synthetic peptide corresponding to the middle portion of the  $A_4$  monomer [SP  $A_4(11-23)$ ] stained APC and ACA and not NFT.

From these experiments we conclude first that NFT, APC and ACA share antigenic determinants and that APC and ACA are antigenically more closely related to each other than to NFT, and second that there are at least two epitopes on the  $A_4$

	% chain	1	2	4	8	9	10	11	15
NFT-AD	trace	Asp · Ala · Glu · Phe · Arg · His · Asp · Ser · Gly · Tyr · Glu · Val · His · His · Gln ...							
	14%	Ala	-----						
	25%		Phe	-----					
	15%				Ser	-----			
	20%					Gly	-----		
	16%						Tyr	-----	
	8%							Val	-----
APC-AD	12%	Asp · Ala · Glu · Phe · Arg · His · Asp · Ser · Gly · Tyr · Glu · Val · His · His · Gln ...							
	64%		Phe	-----					
	16%				Ser	-----			
	8%					Gly	-----		
ACA-AD	100%	Asp · Ala · Glu · Phe · Arg · His · Asp · Ser · Gly · Tyr · Gln · Val · His · His · Gln ...							

**Fig. 4.** N-terminal amino acid sequences of the 4 kd proteins ( $A_{64}$ ) from NFT, APC and ACA. Purified NFT- $A_8$  from three independent experiments (with 6  $\mu$ g, 8  $\mu$ g and 12  $\mu$ g protein) was obtained from h.p.l.c.-purified material as shown in Figure 3. The sequences of NFT- $A_8$  as presented here differ from those of total NFT protein extracts in that the latter show a constant background of proline and glycine residues accounting for ~10% of the material applied onto the glass fiber disk of the sequencer. We interpret this as being due to collagen contaminants which co-purify with the NFT. The sequences of APC- $A_4$  and ACA- $A_4$  are taken from Masters *et al.* (1985) and Glenner and Wong (1984), respectively. The APC- $A_4$  sequence up to residue number 28 is now known (Masters *et al.*, 1985).

monomer: the N-terminal region contains an antigenic site which is exposed in intact NFT and in the  $A_{16}/A_8$  species; the subunits of the APC and ACA fibrils are assembled in such a manner that the central portion of the monomer (at least in the regions of residues 11–23) is exposed. The full unravelling of the antigenic structure of NFT, APC and ACA will prove to be more complex than what has been presented above.

Selkoe and Abraham (1985) recently observed that rabbit antisera to whole NFT also react with isolated APC. Their data therefore confirm our observations that NFT, APC and ACA share antigenic determinants. It is likely that multiple epitopes exist [perhaps related to the N-terminal heterogeneity or to post-translational modification, such as phosphorylation as postulated by Sternberger *et al.*, (1985)] which may partly explain the conflicting results of others who have found that antisera to normal brain components (neurofilaments, microtubules, and vimentin) cross-react with NFT (see, for example, Perry *et al.*, 1985). Monoclonal antibodies which recognize NFT and other normal brain components (Grundke-Iqbal *et al.*, 1985), react by Western blotting with a series of polypeptides derived from NFT solubilized in SDS. These polypeptides range between 16 and 65 kd, and show a remarkable 'step-ladder' effect in which the bands differ equally by 4–5 kd. Since these monoclonal antibodies also recognize the  $A_{64}$  component of a PHF preparation (R. Rubenstein, personal communication), it is likely that these multiple polypeptides differing by 4–5 kd represent the oligomeric state of the NFT subunits in which the  $A_4$  monomer has been dissociated in a step-wise fashion.

#### *There is a non-proteinaceous component in APC and NFT*

Extraction of purified NFT or APC with formic acid leads to the complete removal of the  $A_4$  protein, but leaves behind a visible, insoluble residue. We have analyzed APC by energy dispersive X-ray analysis (both whole APC and their formic acid residues), and found them to contain silicon, aluminum, sodium and calcium as the main non-proteinaceous components (Schröder, Multhaup, Kisters, Masters and Beyreuther, in preparation). While in the center of the APC there is evidence of aluminum silicates containing sodium or other monovalent ions (possibly in the form of 'clay-like' deposits of montmorillonites), at the outer region of the APC, silicon salts are possibly the main inorganic constituent.

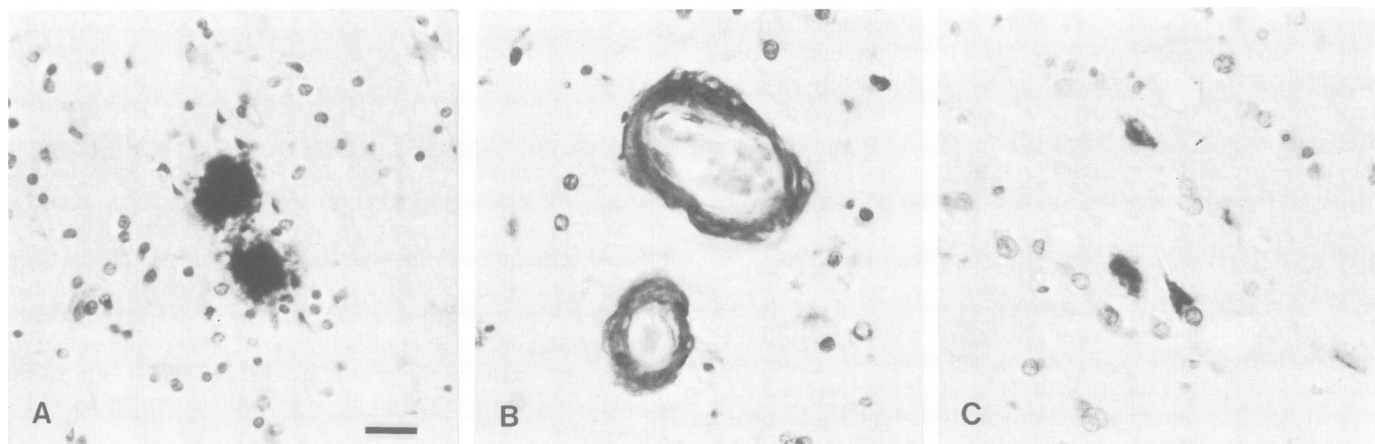


**Fig. 5.** Immunocytochemistry of antibodies raised against whole APC and h.p.l.c.-derived pooled APC- $A_{16}/A_8$  species. Rabbits immunized with whole APC respond by producing antibodies to APC (a) and to the ACA (b). An antiserum raised against APC- $A_{16}/A_8$  species reacts with NFT (c). The sections are of AD cortex, fixed in formalin, embedded in paraffin, using the unlabelled peroxidase-anti-peroxidase technique. Primary antisera were used at a dilution of 1:100. Pre-immune sera at 1:50 dilution were unreactive. (Scale bar 60  $\mu$ m).

### The neuronal origin of the cerebral amyloid

While it has been suggested for many years that NFT, APC and ACA have a common origin, the results outlined above clearly show this to be the case. If one accepts that the relative degrees of N-terminal heterogeneity are a reflection of the age of the deposited amyloid protein, then the conclusion is inescapable that the  $A_4$  protein is derived from the neuron and deposited first in its soma as a tangle and in its axonal terminals as the neuritic degeneration accompanying the plaque. A sequence of events is schematically presented in Figure 6, where after the initial deposition in the neuron, the amyloid spills into the extracellular space to form the APC. Finally, and irregularly, the  $A_4$  protein is deposited around and within blood vessels to form ACA. The alternate hypothesis, that the  $A_4$  protein is derived from an hematogenous precursor, and then transported to the neuron, now seems quite unlikely.

Although the  $A_4$  protein does not show any sequence homology with any of the known components of normal neurofilaments (Geisler *et al.*, 1985), it may be anticipated that  $A_4$  is derived from a component of the cytoskeleton. It may derive from the accumulation of a normal or abnormal gene product (possibly neurofilaments — Gajdusek, 1985) or it may represent a degradation product of some other component of the neuronal cytoskeleton (such as microtubule-associated protein — Gray, 1985).

The size of  $A_4$  is unusual for a primary translational product of a gene, and therefore  $A_4$  is most likely derived from a precursor protein. However, post-translational processing of the putative  $A_4$  precursor does not necessarily depend on a proteolytic activity.

The intriguing association of aluminum silicates with these amyloid proteins (Nikaido *et al.*, 1972; Perl and Brody, 1980) deserves further study. The montmorillonites may form a self-replicating system, structurally resembling  $\beta$ -sheets; they may bind polypeptides with a low content of basic amino acid residues, and are capable of hydrolysing peptide bonds (Weiss, 1981). That the neuronal amyloid proteins can assume paracrystalline arrays (Metzuzals *et al.*, 1981) is consistent with an inorganically based matrix. Although we have no evidence that the montmorillonite-like inorganic residues are involved in the processing of the  $A_4$  protein or its precursor, such a concept does lead to interesting speculation on the origin of aluminum deposits in the NFT of the Guam dementia complex (Garruto *et al.*, 1984), and even into the realm of self-replicating proteins (for example, the generation of amyloid proteins from precursors).

### The structural basis of cerebral amyloid filaments

By electron microscopy, intracellular NFT are composed of paired helical filaments (PHF), on average of larger diameter and of more regular periodicity than the extracellular filaments which form APC and ACA (Merz *et al.*, 1983). If the same protein monomers are the subunits for NFT, APC and ACA, why

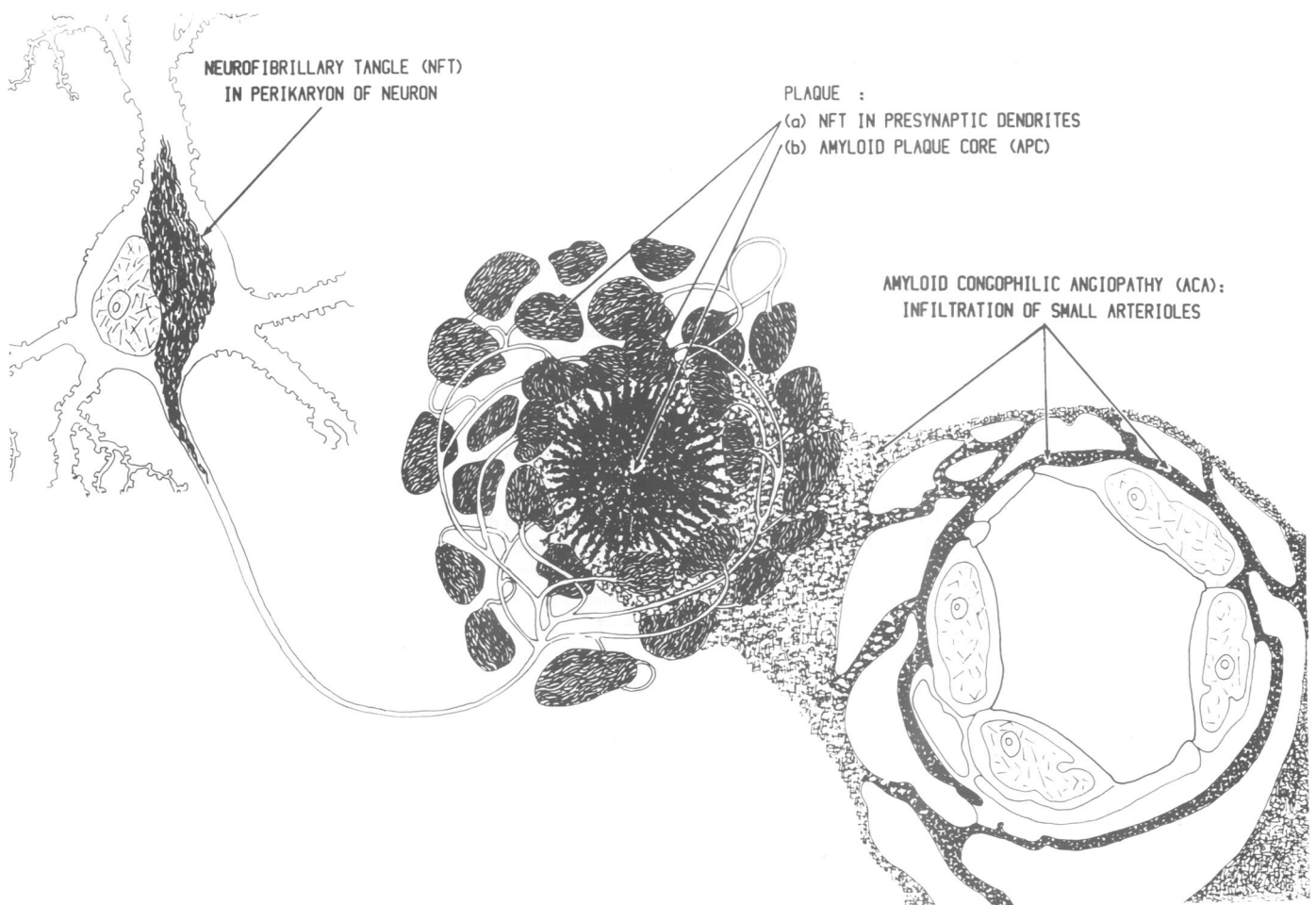


**Fig. 6.** Schematic diagram of the relationships between NFT, APC and ACA. Paired helical filaments are formed first in the intracellular space of the neuron, and coalesce to form neurofibrillary tangles (NFT) in the soma and axonal processes. At the same time or a little later, the same precursor proteins [either in the dimeric ( $A_8$ ) or higher aggregated forms] are deposited in the extracellular space associated with the pre-synaptic axonal processes. These deposited proteins form the amyloid fibrils which may either crystallize within the center of a plaque to form an APC, or the fibrils or their precursor subunits may migrate and accumulate around and within the walls of small blood vessels (ACA).

then are there discernible morphological differences? We suspect that the intracellular NFT protofilaments are assembled from the  $A_4/A_{64}$  units with a different packing density than the extracellular APC/ACA protofilaments. The tightest packing is expected for the full-size ACA- $A_4$  monomers for which no ragged N termini were reported. Indeed, APC and ACA filaments are tightly packed, being straight and single stranded in contrast to the twisted helical filaments or ribbons which comprise the NFT (Wisniewski and Wen, 1985; Wischik *et al.*, 1985). The filaments accumulating in the swollen axonal terminals surrounding the APC are of intermediate size and are heterogeneous (Yoshimura, 1984). Some appear to consist of PHF which are continuous with straight, single-stranded filaments. We suggest that this structural variation is a result of factors such as the N-terminal heterogeneity which is most prominent for NFT- $A_4$ , thus allowing for a greater degree of helicity, or the local environment (ionic strength, pH) in which the filaments are assembled.

It is possible that the His-His sequence (residues 13–14), but not His-7, are responsible for the pH dependency of  $A_4$  aggregation. Protonated histidines promote dissociation, whereas deprotonation favors aggregation, factors which could easily be influenced by the milieu in which the protofilaments are assembled. The suggested  $\beta$ -pleated sheet structures of these amyloid proteins would explain the thread-like aggregation of the  $A_4$  monomers. These monomers, with ~40 residues, are unable by themselves to form a  $\beta$ -barrel structure, the closed-end  $\beta$ -structure of secreted proteins with  $\beta$ -pleated sheets (Schulz and Schirmer, 1984). Such a  $\beta$ -barrel structure would require ~100 residues to form a minimum of six  $\beta$ -strands.  $A_4$  may be considered as half a  $\beta$ -barrel with a high tendency for dimerization to  $A_8$ . The highly stable dimers (which may represent the 'native' or soluble form of the protein in the cytoplasm of neurons) form tetramers. Packing of four tetramers ( $A_{64}$  hexadecamer) would then result in the formation of one segment (disk or sphere) of a protofilament. It has previously been suggested that the amyloid fiber in turn is composed of four or eight protofilaments (Wisniewski and Wen, 1985) or a six-stranded ribbon (Wischik *et al.*, 1985).

#### *The amyloid filaments and proteins of AD are related to the filaments and polypeptides associated with scrapie*

There are several striking similarities between the  $A_4$  proteins of AD and the filaments and polypeptides associated with scrapie. In addition to the previously described morphological resemblances between the APC- and NFT-AD filaments with SAF (Merz *et al.*, 1981; Rubenstein *et al.*, 1985), the chemical inactivation profile of scrapie is similar to the solubility profile for the AD amyloid proteins (Masters *et al.*, 1985). To these, we can now add the strong similarity in amino acid composition between the AD- $A_4$  monomer and the 7-kD deglycosylated scrapie-associated protein (Table I and Multhaup *et al.*, 1985). In length, the AD- $A_4$  monomer is only ~15 amino acids shorter than the scrapie-associated protein. The scrapie-associated protein also has ragged N termini (Multhaup *et al.*, 1985; Oesch *et al.*, 1985).

However there is no sequence homology between AD- $A_4$  and the scrapie polypeptides. The corresponding precursor proteins are clearly distinct. A further difference is that the scrapie-associated protein is glycosylated (to give an apparent mol. wt. of 30 kD) but AD- $A_4$  is not (Masters *et al.*, 1985; Multhaup *et al.*, 1985).

Overall, there are sufficient similarities between the AD and scrapie amyloid filaments and proteins to suspect that they are

derived by mechanisms which have in common the generation of self-aggregating polypeptides of low mol. wt. These mechanisms include mistranslation or altered splicing or processing of translation products. If the scrapie filaments and proteins are an integral part or a direct effect of the infectious agent, it follows that AD is also an infectious process similar to scrapie. Alternatively, it is still conceivable that the amyloid filaments and proteins of both AD and scrapie are pathologic by-products of independent disease processes. This would be consistent with the recent observation that the scrapie-associated protein is encoded by a host gene and is expressed in both normal and infected animals (Oesch *et al.*, 1985). To date, AD remains a non-transmissible disease as judged by long-term animal inoculation studies.

## Materials and methods

### *Isolation of NFT*

NFT were obtained from six cases of AD, using a modification of the method used to purify APC (Masters *et al.*, 1985). The starting material in each case was fresh frozen cerebral cortex, from which the leptomeninges and larger blood vessels had been removed. The cortex was homogenized and extracted in high salt and detergent buffers, digested with pepsin, and centrifuged over a discontinuous sucrose gradient (Masters *et al.*, 1985). The 20–30% sucrose gradient interface was diluted in 50 mM Tris, 1% SDS, 10 mM EDTA, pH 7.6, and incubated at room temperature for 10 min with mixing. After centrifugation at 200 g for 10 min to pellet the APC, the supernatant was centrifuged at 10 000 g for 30 min. The pellet was taken up in the Tris/SDS/EDTA buffer, and layered over a sucrose step gradient (1.0 M, 1.2 M, 1.4 M, 2.0 M sucrose). This gradient is centrifuged at 150 000 g for 2 h at 4°C. NFT are recovered at the 1.4–2.0 M sucrose interface, diluted with distilled water, pelleted at 10 000 g, washed in 2% SDS, then resuspended in Tris-buffered saline and frozen for further analysis. Contaminants, as judged by electron microscopy, consist chiefly of lipofuscin, collagen, amyloid plaque cores and occasional bacteria. Control brains (from individuals without recognizable NFT or APC by light microscopy) were similarly processed, and yielded fractions containing lipofuscin only.

### *Polycrylamide gel electrophoresis*

The formic acid extracts of NFT and APC were lyophilized, dissolved in sample buffer containing 6 M urea but no thiols, and heated for 30 min at 37°C before loading on the gels. Oxidation was achieved with performic acid. The slab gels [15% (w/v) polyacrylamide, 1 mm thick] were made from stock solutions containing 6 M urea and run at 28 mA constant current. The protein bands were stained with Coomassie brilliant blue R.

### *H.p.l.c.*

The protein components of NFT and APC were dissolved in 90% formic acid, lyophilized and re-dissolved in 50  $\mu$ l of h.p.l.c. buffer (0.1% SDS, 150 mM sodium phosphate, pH 6.8). Chromatography was performed on two analytical  $^{125}$ I protein columns (Waters) (30 cm  $\times$  7.8 mm) connected in tandem, with a guard column (3 cm  $\times$  2 mm) filled with  $^{125}$ I bulk packing phase. The flow-rate was 0.2 ml/min, and the protein peaks were detected by absorbance at 214 nm. For amino acid sequencing, protein peaks were lyophilized, then precipitated with methanol (Wessel and Flügge, 1984) to remove excess detergent.

### *Amino acid analysis*

NFT proteins (1–4  $\mu$ g) were hydrolyzed and then analyzed on an automated amino acid analyzer (Beckman 121 M).

### *Protein sequence analysis*

Samples were dissolved in 30  $\mu$ l of formic acid and dried on the glass fiber disks of a gas-liquid solid phase protein sequencer (Applied Biosystems, Model 470A). The filters were pre-loaded with 1.5 mg of pre-conditioned Polybrene (Aldrich). Sequencing was performed as described (Beyreuther *et al.*, 1983).

### *Immunizations and immunocytochemical characterizations*

Rabbits (young adult New Zealand White or Semi-lops) were immunized with various APC or NFT preparations, following the usual schedule of primary inoculation in complete Freund's adjuvant then boosting with antigen in incomplete Freund's adjuvant. Inoculations were made at multiple sites subcutaneously over the rabbit's back.

More than 18 rabbits are being used in these experiments. The antigenic preparations included the following. (i) APC (~2  $\times$  10<sup>5</sup> APC for each dose) which had been (a) left intact; (b) sonicated and coupled to KLH; (c) degraded with alkali (1.0 M NaOH); (d) solubilized in 80% phenol and coupled to KLH; (e)

solubilized in formic acid and coupled to KLH. (ii) The h.p.l.c.-derived fractions corresponding to a pool of the A<sub>16</sub> and A<sub>8</sub> peaks (coupled to KLH) from either APC or NFT starting material. Approximately 5 µg of protein at each inoculation was used. (iii) Synthetic peptides corresponding to residues 1–11 [SPA<sub>4</sub> (1–11)] or residues 11–23 [SPA<sub>4</sub>(11–23)] of the A<sub>4</sub> monomer were made, and coupled to KLH; these synthetic peptides were inoculated in doses of 250 µg.

The rabbits were bled before the immunizations commenced and then after the second and each subsequent boost, and their sera were initially screened by immunocytochemistry, using paraffin-embedded sections of formalin fixed AD or control brain. The sera were used at a dilution of 1:100, using the peroxidase-anti-peroxidase (PAP) technique. Protease digestion (Protease Type VII from *Bacillus amyloliquefaciens*, Sigma P5255, 0.5 mg/ml, at 37°C for 10 min) of the sections was found to enhance the reactivity of some of the antisera towards the APC.

## Acknowledgements

We thank Dr. Neville Hills and the Perth City Mortuary forensic pathologists for providing material; Klaus Neifer, Regine Hanssen, Trudy Parker and Nicola Weinman for skillful technical assistance; Dr. R. Terry for helpful criticism. This research was supported by grants from the National Health and Medical Research Council of Australia (C.L.M.), the Telethon and Royal Perth Hospital Research Foundations (C.L.M.), the Deutsche Forschungsgemeinschaft (SFB 74 to K.B.), the Bundesministerium für Forschung und Technologie (K.B.) and the Fonds der Chemischen Industrie (K.B.).

## References

- Bendheim, P.E., Barry, R.A., DeArmond, S.J., Stites, D.P. and Prusiner, S.B. (1984) *Nature*, **310**, 418–421.
- Beyreuther, K., Bieseler, B., Bovens, J., Dildrop, R., Neifer, K., Stüber, K., Zaiss, S., Ehring, R. and Zabel, P. (1983) in Tschesche, H. (ed.), *Modern Methods in Protein Chemistry*, Walter de Gruyter, Berlin/NY, pp. 303–355.
- DeArmond, S.J., McKinley, M.P., Barry, R.A., Braunfeld, M.B., McColloch, J.R. and Prusiner, S.B. (1985) *Cell*, **41**, 221–235.
- Gajdusek, D.C. (1985) *N. Engl. J. Med.*, **312**, 714–719.
- Garruto, R.M., Fukatsu, R., Yanagihara, R.Y., Gajdusek, D.C., Hook, G. and Fiori, C.E. (1984) *Proc. Natl. Acad. Sci. USA*, **81**, 1875–1879.
- Geisler, N., Plessmann, U. and Weber, K. (1985) *FEBS Lett.*, **182**, 475–478.
- Glenner, G.G. and Wong, C.W. (1984) *Biochem. Biophys. Res. Commun.*, **120**, 885–890.
- Gray, E.G. (1985) *Neuropath. Appl. Neurobiol.*, in press.
- Grundke-Iqbal, I., Wang, G.P., Iqbal, K., Tung, Y.-C. and Wisniewski, H.M. (1985) *Acta. Neuropathol.*, in press.
- Masters, C.L., Gajdusek, D.C. and Gibbs, C.J., Jr. (1981a) *Brain*, **104**, 535–558.
- Masters, C.L., Gajdusek, D.C. and Gibbs, C.J., Jr. (1981b) *Brain*, **104**, 559–587.
- Masters, C.L., Simms, G., Weinman, N.A., Multhaup, G., McDonald, B.L. and Beyreuther, K. (1985) *Proc. Natl. Acad. Sci. USA*, **82**, 4245–4249.
- Merz, P.A., Somerville, R.A., Wisniewski, H.M. and Iqbal, K. (1981) *Acta Neuropathol.*, **54**, 63–74.
- Merz, P.A., Wisniewski, H.M., Somerville, R.A., Bobin, S.A., Masters, C.L. and Iqbal, K. (1983) *Acta. Neuropathol.*, **60**, 113–124.
- Metzals, J., Montpetit, V. and Clapin, D.F. (1981) *Cell Tissue Res.*, **214**, 455–482.
- Multhaup, G., Diring, H., Hilmert, H., Prinz, H. and Beyreuther, K. (1985) *EMBO J.*, **4**, 1495–1501.
- Nikaido, T., Austin, J., Trueb, L. and Rinehart, R. (1972) *Arch. Neurol.*, **27**, 549–554.
- Oesch, B., Westaway, S., Wälchli, M., McKinley, M.P., Kent, S.B.H., Aebersold, R., Barry, R.A., Tempst, P., Teplow, D.B., Hood, L.E., Prusiner, S.B. and Weissmann, C. (1985) *Cell*, **40**, 735–746.
- Perl, D.P. and Brody, A.R. (1980) *Science (Wash.)*, **208**, 297–299.
- Perry, G., Rizzuto, N., Autilio-Gambetti, L. and Gambetti, P. (1985) *Proc. Natl. Acad. Sci. USA*, **82**, 3916–3920.
- Prusiner, S.B., McKinley, M.P., Bowman, D.A., Bolton, D.C., Bendheim, P.E., Groth, D.F. and Glenner, G.G. (1983) *Cell*, **35**, 349–358.
- Rubenstein, R., Kascsak, R.J., Merz, P.A., Wisniewski, H.M., Carp, R.I. and Iqbal, K. (1985) *Brain Res.*, in press.
- Schulz, G. and Schirmer, H. (1984) *Principles of Protein Structure*, published by Springer, Berlin.
- Selkoe, D.J. and Abraham, C. (1985) *Neurology*, **35**, (Suppl. 1), 217.
- Sternberger, N.H., Sternberger, L.A. and Ulrich, J. (1985) *Proc. Natl. Acad. Sci. USA*, **82**, 4274–4276.
- Weiss, A. (1981) *Angew. Chem. Engl. Ed.*, **20**, 850–860.
- Wessel, D. and Flügge, U.I. (1984) *Anal. Biochem.*, **138**, 141–143.
- Wisniewski, H.M., Crowther, R.A., Stewart, M. and Roth, M. (1985) *J. Cell Biol.*, **100**, 1905–1912.
- Wisniewski, H.M. and Wen, G.Y. (1985) *Acta. Neuropathol.*, **66**, 173–176.
- Yoshimura, N. (1984) *Clin. Neuropathol.*, **3**, 22–27.

Received on 7 August 1985